CONTROL OF CARDIAC ALTERNANS USING ELECTRICAL BOUNDARY PACING AND SPATIALLY DISTRIBUTED PERTURBATION CONTROL

Azzam Hazim,[1] Youssef Belhamadia,[2] and Stevan Dubljevic[3]

[1] *Department of Biomedical Engineering, University of Alberta, Edmonton, AB T6G 2V2, Canada*
[2] *Campus Saint-Jean and Department of Mathematics, University of Alberta, Edmonton, AB, T6C 4G9, Canada*
[3] *Deparment of Chemical and Materials Engineering, University of Alberta, Edmonton, AB T6G 2V4, Canada*

Electrical alternans in cardiac Action Potential Duration (APD) have been shown to be a precursor to arrhythmias and sudden cardiac death (SCD). In this work, we study the annihilation of alternans based on an eletro-mechanical model and using boundary pacing and spatially distributed control. The mathematical equations are based on the Nash-Pafilov model (NP), This model includes an additional variable to represent the active stress which is responsible for mechanical deformation and is coupled to the stress equilibrium equation, describing the tissue's mechanics model. An algorithm that combines boundary pacing control and spatially distributed control to annihilate the alternans is implemented using NP model in the limit of small deformation.

I. INTRODUCTION

Electrical alternans is a physiological phenomenon that is a beat-to-beat oscillation (alternation) of the cardiac Action Potential Duration (APD), which is defined as the period of time during which the action potential exceeds the threshold value. Alternans have been shown to be a precursor to arrhythmias [1, 2] and sudden cardiac death (SCD), which is the most common cause of death in the industrialized world. Experimentally, APD alternans is typically observed during rapid pacing at fixed pacing frequency so that beyond a critical pacing frequency the normally periodic response is replaced by a sequence of long and short APDs which is manifested as a variation in the APD (see Fig. 1), the diastolic time interval (DI) in Fig. 1 is defined as the period of time during which the action potential is below the given threshold value.

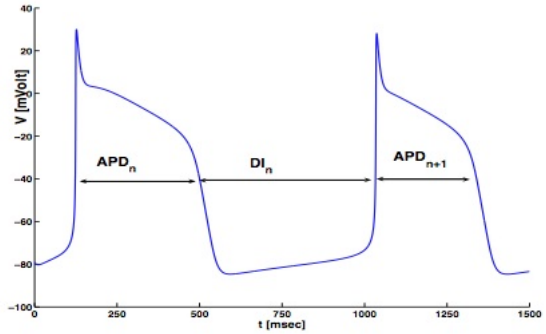

FIG. 1: Time evolution of transmembrane potential in the presence of alternans.

The electrophysiological changes initiate mechanical contraction in the cardiac tissue via excitation-contraction coupling (ECC) while changes in tissue length affect electrophysiological properties via mechanoelectrical feedback (MEF) [3, 4].

Nash-Panfilov (NP) model [5] accounted for electrical and mechanical properties of cardiac tissue by introducing a third variable T_a into the Aliev-Panfilov (AP) model [6], which used two variables to provide a description of excitation for cardiac cells, to link the exitation with contraction. NP model is studied under conditions of small deformations, in which stress equilibrium equation is reduced into linear elasticity equation.

In this work, we develop a control algorithm that combines boundary pacing control and error based feedback control strategy which perturbs the conduction tensor of of NP model to annihilate alternans. Boundary pacing control can be realized by adjusting the stimulation pacing interval subjected by a cardiac system. An electrical boundary control strategy has a finite degree of controllability, such that alternans stabilization in cardiac tissues > 1 cm cannot be achieved [7–9]. To overcome the limitation in controllabity, we added an error based control algorithm, that perturbs conduction tensor of the transmembrane potential of the model in a localized region of the tissue. Perturbing conduction tensor alters the tissue's electric wave profile, and consequently the APD. Through numerical simulations, we demonstrate that the control algorithm can successfully annihilate alternans in the whole cable of cardiac cells.

The outline of the paper is as follows. In section II we present the NP model. section III is devoted to the control and numerical realization of the NP model, and annihilation of cardiac alternans.

II. MATHEMATICAL FORMULATION

The NP mechanical model is based on the finite elastic deformation theory, the reader can refer to [10].

A. Generalities

The Nash-Panfilov (NP) model for the transmembrane potential propagation with electromechanic feedback [5] is given by:

$$\frac{\partial V}{\partial t} = D\frac{\partial}{\partial X_M}\left(\sqrt{C}C^{-1}_{MN}\frac{\partial V}{\partial X_N}\right) + f(V,r) \quad (1)$$

$$\frac{\partial r}{\partial t} = \left(\varepsilon + \frac{\mu_1 r}{\mu_2 + V}\right)(-r - KV(V-b-1)) \quad (2)$$

$$\frac{\partial T_a}{\partial t} = \epsilon(V)(k_{T_a}V - T_a) \quad (3)$$

$$\frac{\partial}{\partial X_M}(S^{MN}F_{jN}) = 0 \quad (4)$$

All parameters and variables are dimensionless, and $f(V,r) = KV(V-a)(1-V) - rV - I_g$. V is the membrane potential, r is the recovery variable, and a is the threshold parameter. $D = 1$ is the diffusion constant, X_k are the fixed reference coordinates, x_k are the material coordinates, C_{MN} is the right Cauchy-Green deformation tensor, S^{MN} is the second Piola-Kirchoff stress tensor, $C = \det(C_{MN})$, it is only present during stretch (i.e. when $\sqrt{C} > 1$), The active tension T_a, increases with V, with a delay fixed by $\epsilon(V)$, given by 0.1 for $V < a$ and 1.0 for $V > a$. k_{Ta} is a parameter that controls the amplitude of T_a, the parameters ε, k, μ_1 and μ_2 have no clear physiological meaning, but are fitted to reproduce the key characteristics of the cardiac tissue [5]. The mechanoelectric feedback is achieved through a stretch-activated current .

$$I_g = G_s(V-1)(\sqrt{C}-1) \quad (5)$$

The Mooney-Rivlin isotropic model is introduced to describe the mechanical properties of the tissue. The total stress is the sum of an active and a passive component.

$$S^{MN} = \frac{1}{2}\left(\frac{\partial W}{\partial C_{MN}} + \frac{\partial W}{\partial C_{NM}}\right) + T_a C^{-1}_{MN} \quad (6)$$

The strain energy function, $W(I_1, I_2)$, for the Mooney-Rivlin model [10] is given by:

$$W(I_1, I_2) = c_1(I_1 - 3) + c_2(I_2 - 3) \quad (7)$$

I_1 and I_2 are the first, and the second invariants of the right Cauchy-Green deformation tensor, c1 and c2 are material constants.

B. Reduction of NP in 1D

Let $x_k = X_k + u_k$, u_k is the displacement variable. In the limit of small deformations, the case where active tension is small compared with passive stress, we will assume $\frac{\partial u_k}{\partial X_M} \ll 1$, $u \ll 1$, and $T_a \ll c_1, c_2$, the elastic

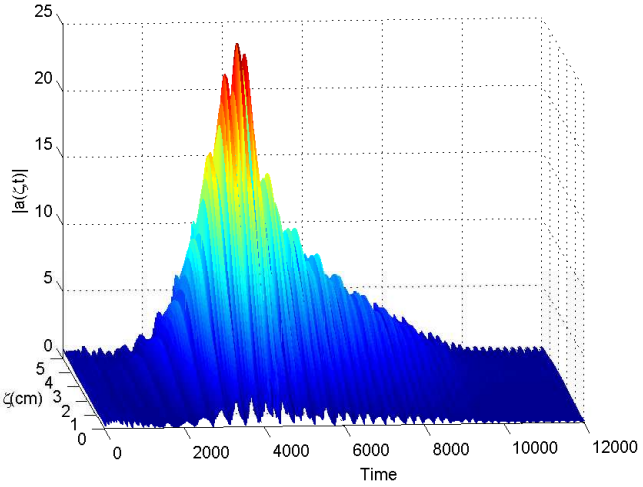

FIG. 2: Amplitude of alternans of NP model. The tissue is paced 62 time units, at which the amplitude of alternans grow until control is applied at $t = 4000$.

equation (4) can be written as $c_1\nabla^2\boldsymbol{u} + c_2\nabla(\nabla\cdot\boldsymbol{u}) + \nabla T_a = 0$. The last equation can be written in 1D as

$$\tilde{c}\frac{\partial^2 u}{\partial X^2} + \frac{\partial T_a}{\partial X} = 0 \quad (8)$$

where $\tilde{c} = c_1 + c_2$. In 1D, the deformation gradient tensor $\mathbf{F}$, the right Cauchy-Green tensor $\mathbf{C}$, and the conduction tensor $\mathbf{D} = \sqrt{C}\mathbf{C}^{-1}$ can be written as

$$\mathbf{F} = \begin{bmatrix} F(X) & 0 & 0 \\ 0 & 1 & 0 \\ 0 & 0 & 1 \end{bmatrix}, \qquad \mathbf{C} = \begin{bmatrix} F^2(X) & 0 & 0 \\ 0 & 1 & 0 \\ 0 & 0 & 1 \end{bmatrix} \quad (9)$$

$$\mathbf{D} = \begin{bmatrix} \frac{1}{F(X)} & 0 & 0 \\ 0 & F(X) & 0 \\ 0 & 0 & F(X) \end{bmatrix} \quad (10)$$

For small deformations, we can linearize $F(X)$ as

$$F(X) = 1 + u(X), \quad (11)$$

III. CONTROL AND NUMERICAL REALIZATION

In this section, we solve Eqs. (1) - (3), and (8) of the NP model, in the limit of small deformation in 1D, to demonstrate alternans annihilation using a control algorithm that combines boundary pacing control and spatially-distributed control. A one dimensional cable of length $L = 5$ cm is considered. As outlined in [5], to determine the scaling factor for the dimensionless time unit, the dimensionless APD obtained from the model

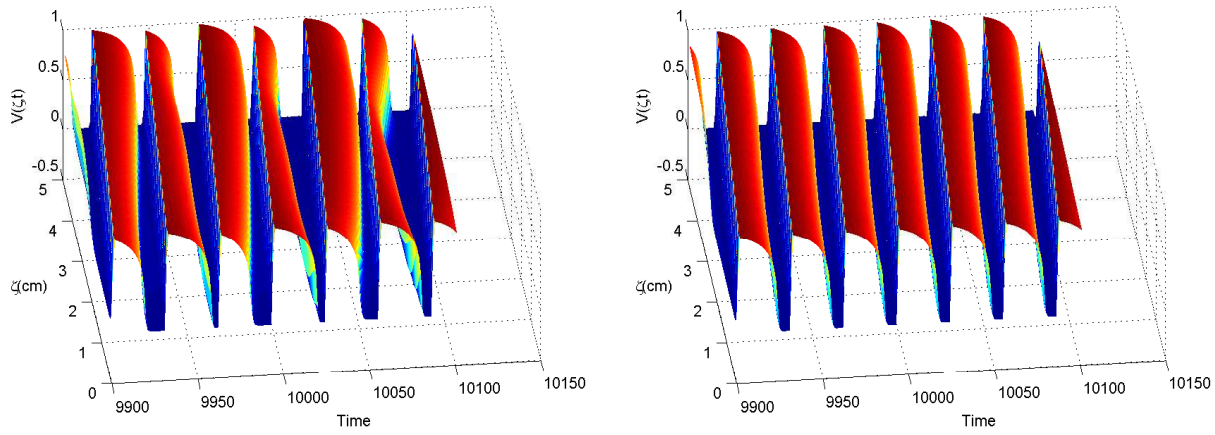

(a) (b)

FIG. 3: Time evolution of membrane potential variable before (a), and after (b) the control is applied.

must be compared to experimental measurements. Scaling factors ranging from 5 ms to 14 ms have been reported [6, 11]. For the dimensionless space variable, 1 dimensionless unit corresponds to 1 mm [6]. The excitation characteristics of the medium was solved using a semi-implicit time integration scheme with $\Delta t = 0.02$ and $\Delta X = 0.1$, and we determine the deformation mechanics of the tissue using second order finite difference scheme. All model parameters used in the simulation are given in Table I. The tissue is paced at the boundary

TABLE I: Parameter values for the electromechanical model

$k = 8$	$a = 0.05$	$\varepsilon = 0.1$	$\mu_1 = 0.12$
$\mu_2 = 0.3$	$k_{Ta} = 0.01$	$\tilde{c} = 16$	$g = 1.6$

to its basic pacing cycle length (PCL), named τ, such that the APD alternates. For the given parameters, τ is found to be 62 time units. Under constant PCL, the amplitude of alternans grows. The APD is measured from the instant V crosses the threshold value during the depolarization phase, until the instant it falls below this value during the repolarization phase. The threshold value is chosen to be 0.02 (in dimensionless units). The amplitude of alternans, $a_n(\zeta)$, is defined as the difference between two consecutive APDs. That is, at a given point in space ζ, $a_n(\zeta) = (APD_n(\zeta) - APD_{n-1}(\zeta))(-1)^n$.

Stabilization of alternans, (see Fig. 2), can be achieved by coupling boundary pacing control and spatially-distributed perturbation control. The boundary pacing control is determined by the dynamic control scheme

$$T^n = \tau + \gamma(APD_n(\zeta = 0) - APD_{n-1}(\zeta = 0)) \quad (12)$$

T^n represents the amount of time between the n-th and $(n+1)$-th stimuli. γ is a tunable constant which define feedback gain of the APD alternation of the basic pacing cycle. In the simulation, $\gamma = 0.325$. For positive γ the second term on the right-hand side of Eq. 12 has the effect of lengthening T^n if the difference of two consecutive APDs is positive. As a result, the following DI, and hence the next APD at the $(n+1)$th beat, is larger using this control scheme. It has been demonstrated by [7, 9, 12] that this pacing control can suppress alternans for the region from the pacing site up to a finite distance ($\leq$ 1cm), beyond that the instabilities grow along the tissue's length and the tissue demonstrates discordant type of alternans but with higher amplitude. A spatially-distributed perturbation control is implemented as follows

$$\frac{\partial V}{\partial t} = \frac{\partial}{\partial X}\left(\left(\frac{1}{F(X)} + \beta e_n(t)\right)\frac{\partial V}{\partial X}\right) + f(V, r) \quad (13)$$

$$e_n(t) = (APD_{\text{ref}} - APD_n) \quad (14)$$

where β is the controller gain. In the simulation, $\beta = 0.05$. The controller acts after the electrical boundary feedback controller stabilizes a finite part of the tissue's length ($\approx$ 1cm). This basic full state feedback algorithm which takes the error $e_n(t)$ (defined in Eq. 14), generated from the difference between APDs references (APD_{ref}) registered at the time t^* (=1479, time we reach basic pacing cycle τ), and the APDs at the n-th stimulus (APD_n), over the length of area under spatially-distributed control, provides a control signal which is applied over the region 1.5-3 cm. The control signal is active only when $e_n(t) > 0$, meaning that the controller only acts on the short-APD, and is turned on when the membrane potential crosses the threshold value at the next APD. This control action alters the tissue's membrane potential through perturbation in **D** is reflected in the membrane potential APD. As shown in Fig. 3, the membrane potential alternate when the control is

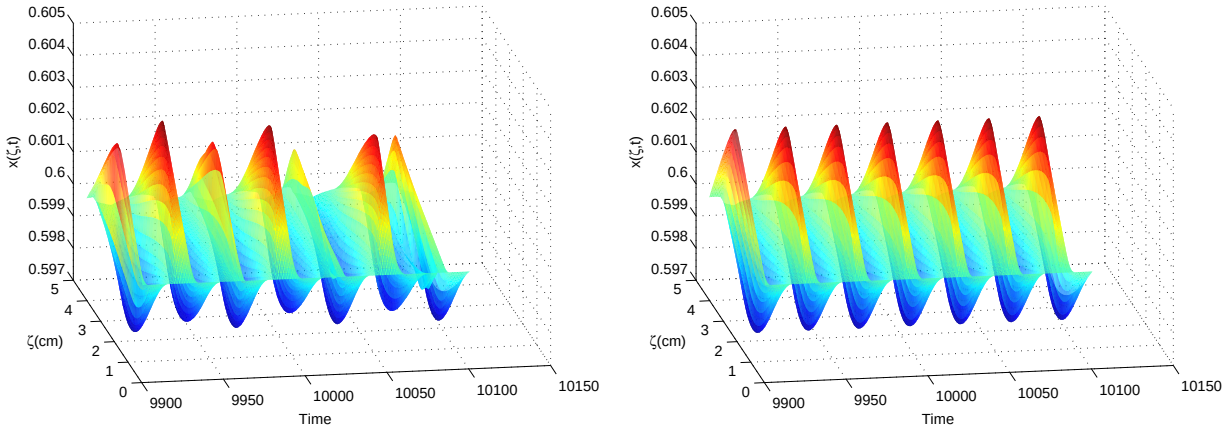

FIG. 4: Time evolution of mechanical deformation variable before (a), and after (b) the control is applied.

not applied, Fig. 3b, and annihilated, Fig. 3b after the control is applied. As shown in Fig. 4, the mechanical deformation variable alternate when the control is not applied, Fig. 4a, and annihilated, Fig. 4a after the control is applied. Although the spatially distributed control is only applied over a localized region of the tissue (1.5 cm), it successfully annihilate alternans along the tissue. Thus, using a model based on the mechanical and electrophysiological properties of the cardiac tissue, it is clearly shown that electrical pacing and spatially distributed perturbations can be used to manipulate the electrical APD in order to suppress alternans.

IV. ACKNOWLEDGMENTS

This research is supported by the Heart and Stroke Foundation of Canada Grant-in-Aid (GIA).

[1] L. Makarov and V. Komoliatova, "Microvolt t-wave alternans during holter monitoring in children and adolescents," *ANN Noninvas Electro*, vol. 15, no. 2, pp. 138–144, 2010.

[2] S. M. Narayan, "T-wave alternans and human ventricular arrhythmias: What is the link?" *J Am Coll Cardiol*, vol. 49, no. 3, pp. 347–349, 2007.

[3] I. Kiseleva, K. Wagner, H. Theres, A. Ladhoff, H. Scholz, J. Gunther, M. Lab, and B. Echebarria, "Mechano-electric feedback after left ventricular infarction in rats," *Cardiovascular*, vol. 45, pp. 370–378, 2000.

[4] P. Kohl and U. E. Ravens, "Special issue on mechano-electric feedback and cardiac arrhythmias," *Progress in Biophysics and Molecular*, vol. 82, 2003.

[5] M. P. Nash and A. V. Panfilov, "Electromechanical model of excitable tissue to study reentrant cardiac arrhythmias," *Prog Biophys Mol Bio*, vol. 85, no. 2-3, pp. 501 – 522, 2004.

[6] R. R. Aliev and A. V. Panfilov, "A simple two-variable model of cardiac excitation," *Chaos Soliton Frac*, vol. 7, no. 3, pp. 293–301, 1996.

[7] D. J. Christini *et al.*, "Control of electric alternans in canine cardiac purkinje fibers," *Phys Rev Lett*, vol. 96, p. 104101, 2006.

[8] J. J. Fox *et al.*, "Spatiotemporal transition to conduction block in canine ventricle," *Circ Res*, vol. 289, 2002.

[9] B. Echebarria and A. Karma, *Chaos*, vol. 12, pp. 923 – 930, 2002.

[10] Y. Fung and P. Tong, "Classical and computational solid mechanics."

[11] A. V. Panfilov, "Spiral breakup as a model of ventricular fibrillation," *Chaos*, vol. 8, pp. 57–64, 1998.

[12] S. Dubljevic, S. F. Lin, and P. D. Christofides, "Studies on feedback control of cardiac alternans," *Comput Chem Eng*, vol. 32, no. 9, pp. 2086 – 2098, 2008.